



Ultraviolet and blue up-conversion fluorescence of $\text{NaY}_{0.793-x}\text{Tm}_{0.007}\text{Yb}_{0.2}\text{Gd}_x\text{F}_4$ phosphors

Chunyan Cao^{a,*}, Xianmin Zhang^b, Minglun Chen^a, Weiping Qin^c, Jisen Zhang^d

^a College of Mathematics and Physics, Jinggangshan University, Ji'an 343009, PR China

^b Department of Physics, Liaoning University, Shenyang 110036, PR China

^c State Key Laboratory on Integrated Optoelectronics, College of Electronic Science and Engineering, Jilin University, Changchun 130012, PR China

^d Key Laboratory of Excited State Processes, Changchun Institute of Optics, Fine Mechanics and Physics, Chinese Academy of Sciences, Changchun 130033, PR China

ARTICLE INFO

Article history:

Received 27 March 2010

Received in revised form 27 May 2010

Accepted 30 May 2010

Available online 11 June 2010

PACS:

42.65.-k

78.55.-m

Keywords:

Up-conversion

Ultraviolet

Blue

Fluorescence

ABSTRACT

The $\text{NaY}_{0.793-x}\text{Tm}_{0.007}\text{Yb}_{0.2}\text{Gd}_x\text{F}_4$ ($x=0.1, 0.2, 0.3$) phosphors were synthesized through a combinational method of co-precipitation and argon atmosphere annealing procedures. Crystallizations of the phosphors were characterized by X-ray diffraction (XRD) analysis. Under a 980-nm continuous wave laser diode (LD) excitation, the phosphors exhibited UV UC fluorescence of Gd^{3+} peaking at 246.4, 252.8, 276.2, 279.2, 305.8, and 311.4 nm, respectively. At the same time, UV UC fluorescence centering at 264.6, 289.6, 344.2, 361.0 nm and blue UC fluorescence peaking at 449.8 and 472.8 nm of Tm^{3+} were observed. The up-converted process analysis indicated that the energy transfer from Tm^{3+} to Gd^{3+} played a vital role in UV UC emissions of Gd^{3+} . And the optical property analysis suggested that both excitation powers and host material compositions had great effects not only on UV UC fluorescence of Gd^{3+} , but also on UV and blue UC fluorescence of Tm^{3+} .

© 2010 Elsevier B.V. All rights reserved.

1. Introduction

Up-conversion (UC) is one of physical mechanisms for changing the frequency of light, where lower energy light (usually near-infrared (NIR) or infrared (IR)) is converted to high energy light (ultraviolet (UV) or visible) via multistep absorptions, energy transfer (ET) processes, etc. For benefits of intrinsic energy levels matching of certain rare earth (RE) ions and ample availabilities of laser diodes (LDs) in IR range, frequency UC is an important process in optical generation within RE-doped materials. RE-doped up-converted materials have been widely studied because of their potential applications, such as optical data storage, color displays, IR sensors, environmental monitoring, biosensors, and so on [1–5]. Gd^{3+} compounds, such as Gd_2SiO_5 [6], Gd_2O_3 [7], LiGdF_4 [8], and GdBO_3 [9], have a wide range of applications and are extensively studied and used where Gd^{3+} ions serve as host material ions, activator ions, or sensitizer ions. However, UC fluorescence of Gd^{3+} has been rarely studied for large energy gap between the ground state $^8\text{S}_{7/2}$ and the first excited state $^6\text{P}_{7/2}$ ($\sim 32,000\text{ cm}^{-1}$). In Ref. [10] the researchers firstly used green lasers (546 and 522 nm) as pump

lights and observed UC emissions of Gd^{3+} in CsMgCl_3 . Cao et al. reported the $^6\text{I}_J$ and $^6\text{P}_J$ states to the ground state $^8\text{S}_{7/2}$ emissions of Gd^{3+} in YF_3 with a 980-nm LD as excitation source in 2008 [11]. Later, Qin et al. observed the $^6\text{D}_J$ levels to the $^8\text{S}_{7/2}$ level emissions in GdF_3 under the same measurement conditions [12]. Subsequently, Chen et al. reported the near vacuum UV (VUV) UC fluorescence of Gd^{3+} in NaGdF_4 powders under a 974-nm LD excitation [13]. To the best of our knowledge, there were few reports about Gd^{3+} fluorescence based on NaYF_4 host materials.

In this article, we presented an observation of UV and blue UC fluorescence of Gd^{3+} and Tm^{3+} ions in $\text{NaY}_{0.793-x}\text{Tm}_{0.007}\text{Yb}_{0.2}\text{Gd}_x\text{F}_4$ ($x=0.1, 0.2, 0.3$) phosphors with a 980-nm semiconductor continuous wave LD as excitation source. In the studied $\text{Yb}^{3+}\text{-Tm}^{3+}\text{-Gd}^{3+}$ system exciting by a 980-nm LD, Yb^{3+} ions serving as primary sensitizers and Tm^{3+} ions acting as secondary sensitizers continuously transferred energies to Gd^{3+} resulting in UV UC fluorescence of Gd^{3+} . Tm^{3+} acted as activators in its own UV and blue UC fluorescence at the same time.

2. Experimental

$\text{NaY}_{0.793-x}\text{Tm}_{0.007}\text{Yb}_{0.2}\text{Gd}_x\text{F}_4$ ($x=0.1, 0.2, 0.3$) phosphors were synthesized as following. In a typical procedure for preparation of $\text{NaY}_{0.593}\text{Tm}_{0.007}\text{Yb}_{0.2}\text{Gd}_{0.2}\text{F}_4$, two clear solutions A and B were prepared firstly. 10 mmol stoichiometric amounts of Y_2O_3 , Yb_2O_3 , Gd_2O_3 , and Tm_2O_3 were dissolved in dilute HCl at elevated temper-

* Corresponding author. Tel.: +86 796 8100489; fax: +86 796 8124959.
E-mail address: caoyan.80@126.com (C. Cao).

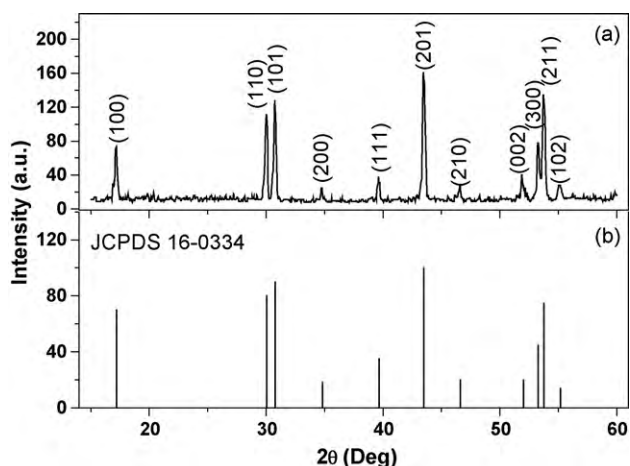


Fig. 1. XRD patterns of (a) $\text{NaY}_{0.593}\text{Tm}_{0.007}\text{Yb}_{0.2}\text{Gd}_{0.2}\text{F}_4$ and (b) the standard data.

ature to form clear solution A. Meanwhile, solution B was prepared by dissolving 30 mmol NH_4HF_2 in deionized water. Then, solution B was added dropwise into solution A to form turbid solution C while stirring with a magnetic force stirrer. After being vigorously stirred for more than 0.5 h, solution C was washed with deionized water via centrifugation at least 3 times. After dried in vacuum at 55°C for 10 h, the resulting white powder was obtained. However, the white powder had hardly UC fluorescence under 980-nm excitation. 20 mmol NaF mixed with the white powder were ground for 0.5 h using an agate mortar. After being heated at 500°C for 1 h in an argon atmosphere, the phosphor $\text{NaY}_{0.593}\text{Tm}_{0.007}\text{Yb}_{0.2}\text{Gd}_{0.2}\text{F}_4$ was obtained and emitted bright blue and intense UV light under 980-nm excitation. Other phosphors $\text{NaY}_{0.793-x}\text{Tm}_{0.007}\text{Yb}_{0.2}\text{Gd}_x\text{F}_4$ ($x=0.1$ and 0.3) were prepared in a similar manner to that for $\text{NaY}_{0.593}\text{Tm}_{0.007}\text{Yb}_{0.2}\text{Gd}_{0.2}\text{F}_4$.

Crystallization phase identification was carried out by X-ray diffraction (XRD) with a powder diffractometer (Model Rigaku RU-200b) using nickel-filtered $\text{CuK}\alpha$ radiation ($\lambda = 1.5406 \text{ \AA}$). Using a 980-nm semiconductor continuous wave LD with a maximum power of 2 W as excitation source, UC fluorescence spectra were recorded with a fluorescence spectrophotometer (Hitachi F-4500). All measurements were performed at room temperature.

3. Results and discussion

3.1. Characterization

Fig. 1(a) shows XRD pattern of the phosphor $\text{NaY}_{0.593}\text{Tm}_{0.007}\text{Yb}_{0.2}\text{Gd}_{0.2}\text{F}_4$. Fig. 1(b) is literature data pub-

lished by the Joint Committee on Powder Diffraction Standard (JCPDS 16-0334) which is in hexagonal phase with space group $P6_3/m$ (176). Comparing the two patterns, one can learn that all diffraction peaks can be easily indexed to those of standard data. From narrowed peaks in Fig. 1(a), we infer that the phosphor crystallized well.

3.2. UC fluorescence spectra

Under 980-nm excitation with pumping power about 650 mW, the phosphor $\text{NaY}_{0.593}\text{Tm}_{0.007}\text{Yb}_{0.2}\text{Gd}_{0.2}\text{F}_4$ has intense UV and bright blue UC fluorescence in the wavelength range of 240–510 nm as shown in Fig. 2. For clarity, the spectra are separately placed in the wavelength range of 240–320 nm (Fig. 2(a)) and 320–510 nm (Fig. 2(b)), respectively. Fig. 2(a) is mainly UC fluorescence of Gd^{3+} . The intensity is magnified 5 times in the wavelength range of 240–270 nm for the fluorescence is relatively weak. The emissions which peaked at 246.4 and 252.8 nm are assigned to transitions from ${}^6\text{D}_{7/2}, {}^6\text{D}_{9/2} \rightarrow {}^8\text{S}_{7/2}$ of Gd^{3+} , respectively [12]. The emission that centered at 264.6 nm comes from ${}^3\text{P}_2 \rightarrow {}^3\text{H}_6$ transition of Tm^{3+} . Emissions in the wavelength range of 270–282 nm (two main peaks centered at 276.2 and 279.2 nm) come from ${}^6\text{I}_J \rightarrow {}^8\text{S}_{7/2}$ transitions of Gd^{3+} . The emission centered at 289.6 nm is assigned to the ${}^1\text{I}_6 \rightarrow {}^3\text{H}_6$ transition of Tm^{3+} . And, emissions which peaked at 305.8 and 311.4 nm originate from ${}^6\text{P}_{5/2}, {}^6\text{P}_{7/2} \rightarrow {}^8\text{S}_{7/2}$ transitions of Gd^{3+} , respectively. Fig. 2(b) shows UC fluorescence spectrum of Tm^{3+} in the wavelength range of 320–510 nm. The emission that peaked at 344.2 nm comes from ${}^1\text{I}_6 \rightarrow {}^3\text{F}_4$ transition. Emissions which centered at 361.0 and 449.8 nm are attributed ${}^1\text{D}_2 \rightarrow {}^3\text{H}_6, {}^3\text{F}_4$ transitions, respectively. And the emission that peaked at 472.8 nm originates from ${}^1\text{G}_4 \rightarrow {}^3\text{H}_6$ transition.

3.3. Up-converted processes

Fig. 3 describes schematically possible up-converted processes in energy level diagrams of Yb^{3+} , Tm^{3+} , and Gd^{3+} [14,15]. In a Tm^{3+} - Yb^{3+} - Gd^{3+} co-existing system under 980-nm excitation, Yb^{3+} ions successively transfer energies to Tm^{3+} ions to populate their ${}^3\text{H}_5$, ${}^3\text{F}_3$ (${}^3\text{F}_2$), and ${}^1\text{G}_4$ levels in turn [16]. The ${}^1\text{D}_2$ level cannot be populated directly through ET ${}^2\text{F}_{5/2} \rightarrow {}^2\text{F}_{7/2}$ (Yb^{3+}): ${}^1\text{G}_4 \rightarrow {}^1\text{D}_2$ (Tm^{3+}) for large energy mismatch ($\sim 3500 \text{ cm}^{-1}$) in the ET. And the ${}^1\text{D}_2$ level can be populated through cross relaxation ET (CRET) ${}^3\text{F}_3 \rightarrow {}^3\text{H}_6$:

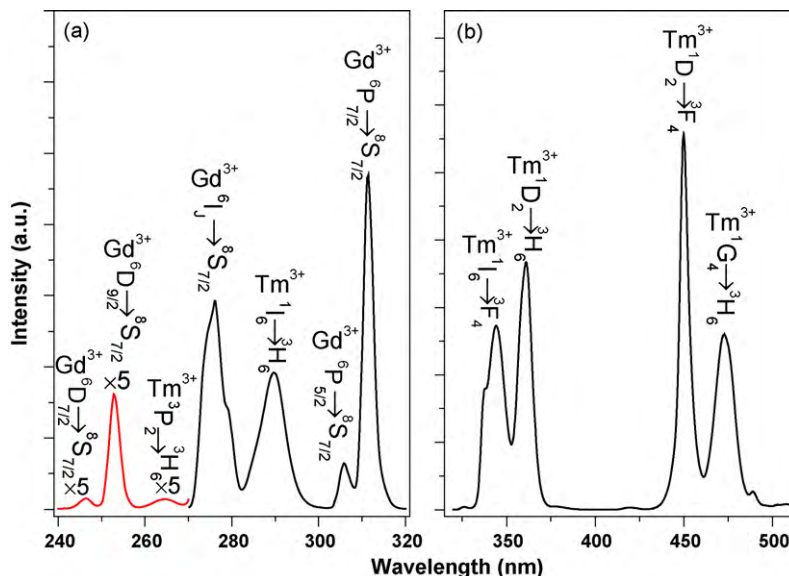


Fig. 2. Up-conversion fluorescence of phosphor $\text{NaY}_{0.593}\text{Tm}_{0.007}\text{Yb}_{0.2}\text{Gd}_{0.2}\text{F}_4$.

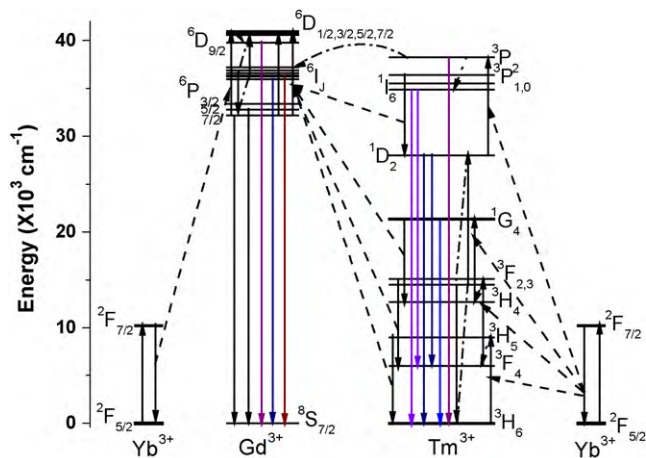


Fig. 3. Energy level diagrams of Gd^{3+} , Yb^{3+} , Tm^{3+} ions, and possible up-converted processes.

${}^3F_3 \rightarrow {}^1D_2$ (Tm^{3+}) [17,18]. Further, the 3P_2 (Tm^{3+}) level is populated by ET ${}^2F_{5/2} \rightarrow {}^2F_{7/2}$ (Yb^{3+}): ${}^1D_2 \rightarrow {}^3P_2$ (Tm^{3+}). Then, some of Tm^{3+} ions in the 3P_2 state make radiative transition of ${}^3P_2 \rightarrow {}^3H_6$ and some of them relax rapidly to the 1I_6 level resulting in ${}^1I_6 \rightarrow {}^3H_6, {}^3F_4$ transitions. Gd^{3+} in the ground state cannot absorb 980-nm photons directly for the large energy gap between the first excited state and the ground state. However, the 6I_J -excited states of Gd^{3+} can be populated through ET ${}^3P_2 \rightarrow {}^3H_6$ (Tm^{3+}): ${}^8S_{7/2} \rightarrow {}^6I_J$ (Gd^{3+}). Nonradiative relaxation probabilities of ${}^6I_J \rightarrow {}^6P_J$ are larger than radiative transition probability of ${}^6I_{7/2} \rightarrow {}^8S_{7/2}$ at room temperature [19], which results in populating ${}^6P_{5/2}$ and ${}^6P_{7/2}$ levels efficiently. And the 6D_J levels of Gd^{3+} ions will be populated further. As reported in Ref. [12], three mechanisms should be considered in populating the 6D_J levels, viz. excited state absorption (ESA), CRET, and ET. Due to their appropriate energy matching conditions, ET ${}^2F_{5/2} \rightarrow {}^2F_{7/2}$ (Yb^{3+}): ${}^6P_{7/2} \rightarrow {}^6D_J$ (Gd^{3+}) should be the dominant process in populating the 6D_J levels because of high concentration of Yb^{3+} ions in phosphors and strong absorption of Yb^{3+} at about 980 nm.

3.4. UC fluorescence properties

UC fluorescence properties of the phosphors are studied in detail in the article. Fig. 4 is excitation power dependent UC fluorescence spectra of phosphor $NaY_{0.593}Tm_{0.007}Yb_{0.2}Gd_{0.2}F_4$ in the wavelength range of 240–320 nm. As is illustrated in the figure, the 252.8 nm

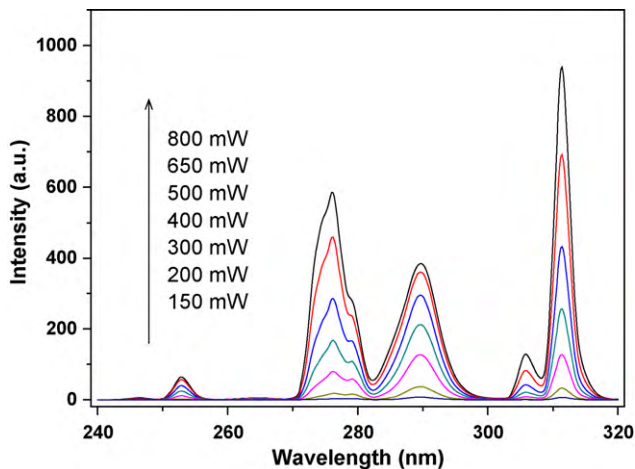


Fig. 4. Excitation power dependent up-conversion fluorescence spectra of phosphor $NaY_{0.593}Tm_{0.007}Yb_{0.2}Gd_{0.2}F_4$.

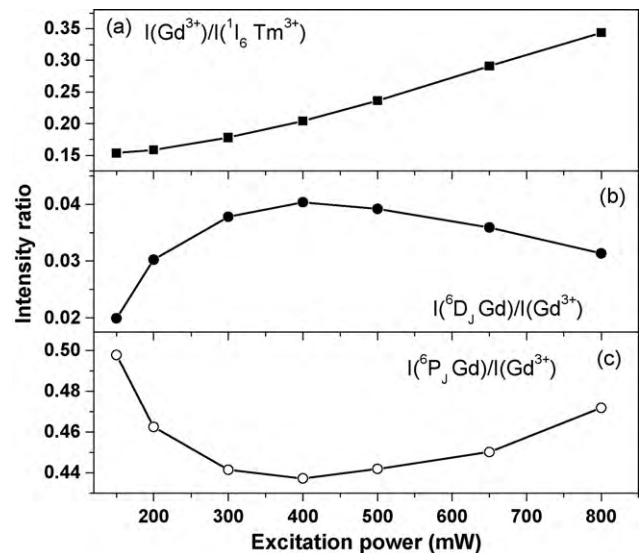


Fig. 5. Intensity ratio plots of (a) $I(Gd^{3+})/I({}^1I_6 Tm^{3+})$, (b) $I({}^6D_J Gd^{3+})/I(Gd^{3+})$, (c) $I({}^6P_J Gd^{3+})/I(Gd^{3+})$.

emission of Gd^{3+} appears and gradually gets stronger when excitation powers increase from 150 to 800 mW. At the same time, the 6I_J level emissions of 276.8 nm predominate over that 279.0 nm emission gradually. In general, populations on two near levels follow quasi-thermal equilibrium and the higher energy level can be populated from the lower level by thermal excitation [20]. With thermal equilibrium of population at the two levels and ignoring effects of self-absorption of fluorescence, the fluorescence intensity ratio between the higher level and the lower level can be expressed as: $R = C \exp[-\Delta E/(kT)]$, where ΔE is the energy gap between the two levels, k is the Boltzmann constant, T is the absolute temperature, and C is a constant about the two levels [21]. The energy difference between fluorescence peaking at 276.8 and 279.0 nm is only $\sim 284 \text{ cm}^{-1}$. This energy separation allows the higher level to be populated from the lower level of 6I_J levels by thermal excitation and quasi-thermal equilibrium occurs between 6I_J levels, which lead to variations of UC fluorescence spectra.

In addition, integrated UC fluorescence intensity ratios of the phosphors are researched to value the ET between Gd^{3+} and Tm^{3+} , too. Fig. 5 shows relative integrated fluorescence intensity ratios of phosphor $NaY_{0.593}Tm_{0.007}Yb_{0.2}Gd_{0.2}F_4$ corresponding to excitation powers. Fig. 5(a) is the ratio plot of all UC fluorescence of Gd^{3+} (${}^6D_J, {}^6I_J, {}^6P_J \rightarrow {}^8S_{7/2}$) (signed as $I(Gd^{3+})$) to those of 1I_6 (${}^1I_6 \rightarrow {}^3H_6, {}^3F_4$) fluorescence (signed as $I({}^1I_6 Tm^{3+})$) of Tm^{3+} with increase of excitation powers, which is always increasing meaning that the ET from Tm^{3+} to Gd^{3+} gets efficient with excitation power increasing. Fig. 5(b) shows the ratio curve of 6D_J fluorescence (written as $I({}^6D_J Gd^{3+})/I(Gd^{3+})$), which has the maximum value when the excitation power is 400 mW. And Fig. 5(c) is the ratio curve of 6P_J fluorescence (written as $I({}^6P_J Gd^{3+})/I(Gd^{3+})$), which firstly decreases then gradually increases with excitation powers increasing. Differing from ratio variations of $I({}^6D_J Gd^{3+})/I(Gd^{3+})$, ratio of $I({}^6P_J Gd^{3+})/I(Gd^{3+})$ reaches the minimum at 400 mW. In phosphors, the local thermal effect caused by laser irradiation is evident under high power excitation [22], which leads to the temperature of phosphors increasing. The variations of intensity ratios have relations with phosphor temperatures which increase with the increasing excitation power. When excitation power increases, the ET from Tm^{3+} to Gd^{3+} becomes efficient while temperatures of phosphor increase, which will damp further ET to populate the upper 6D_J levels. As a result the profiles of spectra vary like those presented in the above text.

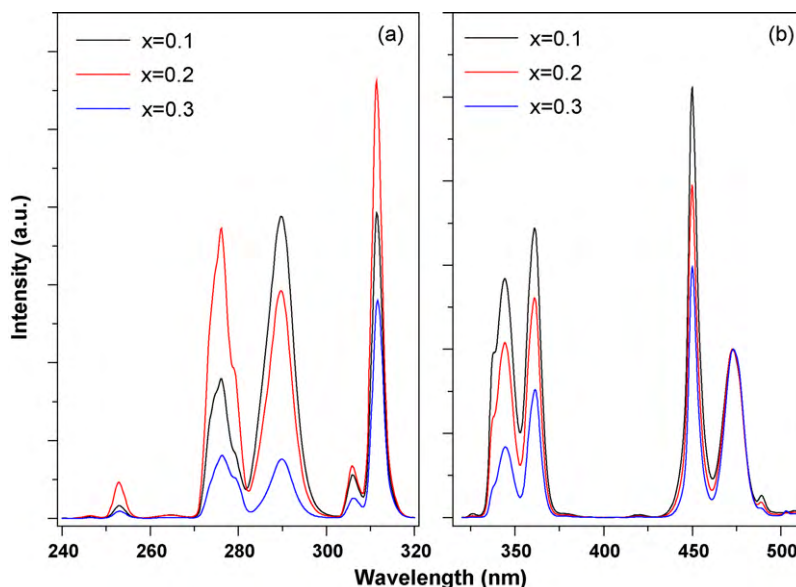


Fig. 6. Up-conversion fluorescence spectra of phosphors $\text{NaY}_{0.793-x}\text{Tm}_{0.007}\text{Yb}_{0.2}\text{Gd}_x\text{F}_4$ ($x=0.1, 0.2, 0.3$).

In order to obtain strong UV UC fluorescence of Gd^{3+} , we optimize host materials by adjusting their components. Previous investigation indicates that NaYF_4 sensitized by Yb^{3+} is the best host material for UC fluorescence with moderate excitation intensities in the NIR [23–27]. Fig. 6 shows UC fluorescence spectra of phosphors $\text{NaY}_{0.793-x}\text{Tm}_{0.007}\text{Yb}_{0.2}\text{Gd}_x\text{F}_4$ ($x=0.1, 0.2, 0.3$) which are all recorded under the same measurement conditions (Em slit=1.0 nm, high voltage of photomultiplier tube (PMT)=700 V, excitation power=650 mW). Fluorescence from Gd^{3+} firstly increases then decreases in phosphors with x value changes from 0.1 to 0.3 while $^1\text{I}_6 \rightarrow ^3\text{H}_6$ (Tm^{3+}) emission decreases constantly, which is shown in Fig. 6(a). The phosphor with $x=0.1$ has the strongest $^1\text{I}_6 \rightarrow ^3\text{H}_6$ emission of Tm^{3+} and all Gd^{3+} emissions are moderate in the three phosphors. When Gd^{3+} concentration is 20%, all emissions of Gd^{3+} are strongest and Tm^{3+} emission $^1\text{I}_6 \rightarrow ^3\text{H}_6$ becomes weaker. All emissions of Gd^{3+} and Tm^{3+} are weakest when Gd^{3+} concentration reaches 30%. The relatively UC fluorescence intensity variations of Gd^{3+} and Tm^{3+} prove the ET from Tm^{3+} to Gd^{3+} . The experimental results indicate that Gd^{3+} obtains the maximum fluorescence when its concentration is 20% when Tm^{3+} concentration is fixed. High or low concentration has no benefit on UC fluorescence of Gd^{3+} but that is not the same to Tm^{3+} . Fig. 6(b) is spectra in the wavelength range of 320–510 nm which has only Tm^{3+} fluorescence. All emissions become weaker with Gd^{3+} concentration increasing meaning higher concentration of Gd^{3+} resulting weaker fluorescence of Tm^{3+} . In a word, the variations of UC fluorescence spectra in Fig. 6 indicate ET from Tm^{3+} to Gd^{3+} occurring. The ET from Tm^{3+} to Gd^{3+} and concentrations of Gd^{3+} play vital roles on UV UC fluorescence of Gd^{3+} . Furthermore, the analysis suggests that NaGdF_4 is not a good UC host material as NaYF_4 sensitized by Yb^{3+} for Tm^{3+} UC emissions.

4. Conclusions

In conclusion, through an easy combinational method of coprecipitation and argon atmosphere annealing procedures, the $\text{NaY}_{0.793-x}\text{Tm}_{0.007}\text{Yb}_{0.2}\text{Gd}_x\text{F}_4$ ($x=0.1, 0.2, 0.3$) phosphors were synthesized. XRD analysis indicated that the phosphors were in hexagonal phases. The UV and blue UC fluorescence spectra studies were performed on the phosphors with a 980-nm LD as the excitation source. The strongest Tm^{3+} fluorescence was obtained when

$x=0.1$, while the strongest Gd^{3+} fluorescence was obtained with $x=0.2$ in the three phosphors. The experimental results indicated that the excitation powers and the composition of the materials had great effects on the UC fluorescence of Gd^{3+} and Tm^{3+} . The study suggested that the phosphors might be used as UV and blue UC fluorescence materials.

Acknowledgements

This work was financially supported by the Natural Science Foundation of Jiangxi Province (Granted Nos. 2009GQW0010, 2009GZW0012), the Science and Technology Program of Department of Education of Jiangxi Province (Granted No. GJJ10203), the National Natural Science Foundation of China (Granted Nos. 10847141, 10774142, and 10874058), and the Research Program of Liaoning Educational Department (2009A308).

References

- [1] X. Zhang, C. Serrano, E. Daran, F. Lahoz, G. Lacostc, A. Munoz-Yague, Phys. Rev. B 62 (2000) 4446.
- [2] F. Auzel, Chem. Rev. 104 (2004) 139.
- [3] H. Ping, D.Q. Chen, Y.L. Yu, Y.S. Wang, J. Alloys Compd. 490 (2010) 74.
- [4] G.F. Wang, Q. Peng, Y.D. Li, J. Am. Chem. Soc. 131 (2009) 14200.
- [5] S.J. Zeng, G.Z. Ren, Q.B. Yang, J. Alloys Compd. 493 (2010) 476.
- [6] K. Takagi, T. Fukazaw, Appl. Phys. Lett. 42 (1983) 43.
- [7] H. Guo, N. Dong, M. Yin, W.P. Zhang, L.R. Lou, S.D. Xia, J. Phys. Chem. B 108 (2004) 19205.
- [8] R.T. Wegh, H. Donker, K.D. Oskam, A. Meijerink, Science 283 (1999) 663.
- [9] Q.Y. Zhang, C.H. Yang, Z.H. Jiang, X.H. Ji, Appl. Phys. Lett. 90 (2007) 061914.
- [10] A.R. Gharavi, G.L. McPherson, J. Opt. Soc. Am. B 11 (1994) 913.
- [11] C.Y. Cao, W.P. Qin, J.S. Zhang, Y. Wang, P.F. Zhu, G.D. Wei, G.F. Wang, R. Kim, Opt. Lett. 33 (2008) 857.
- [12] W.P. Qin, C.Y. Cao, L.L. Wang, J.S. Zhang, D.S. Zhang, K.Z. Zheng, Y. Wang, G.D. Wei, G.F. Wang, P.F. Zhu, R. Kim, Opt. Lett. 33 (2008) 2167.
- [13] G.Y. Chen, H.J. Liang, H.C. Liu, G. Somesfalean, Z.G. Zhang, Opt. Express 17 (2009) 16366.
- [14] W.T. Carnall, P.R. Fields, K. Rajnak, J. Chem. Phys. 49 (1968) 4412.
- [15] W.T. Carnall, P.R. Fields, K. Rajnak, J. Chem. Phys. 49 (1968) 4424.
- [16] F. Auzel, C. R. Acad. Sci. Paris 262 (1966) 1016.
- [17] R.J. Thrash, L.F. Johnson, J. Opt. Soc. Am. B 11 (1994) 881.
- [18] M.A. Noginov, M. Curley, P. Venkateswarlu, A. Williams, H.P. Jensen, J. Opt. Soc. Am. B 14 (1997) 2126.
- [19] J. Sytsma, G.F. Imbush, G. Blasse, J. Phys. Condens. Matter 2 (1990) 5171.
- [20] E. Maurice, G. Monnom, A. Saissy, D.B. Ostrowsky, G.W. Baxter, Opt. Lett. 19 (1994) 990.
- [21] B. Dong, D.P. Liu, X.J. Wang, T. Yang, S.M. Miao, C.R. Li, Appl. Phys. Lett. 90 (2007) 181117.

- [22] Y.Q. Lei, H.W. Song, L.M. Yang, L.X. Yu, Z.X. Liu, G.H. Pan, X. Bai, L.B. Fan, *J. Chem. Phys.* 123 (2005) 174710.
- [23] K. Krämer, D. Biner, G. Frei, H. Güdel, M. Hehlen, S. Lüthi, *Chem. Mater.* 16 (2004) 1244.
- [24] S.Y. Tan, P.P. Yang, N. Niu, S.L. Gai, J. Wang, X.Y. Jing, J. Lin, *J. Alloys Compd.* 490 (2010) 684.
- [25] Y. Wei, F.Q. Lu, X.R. Zhang, D.P. Chen, *J. Alloys Compd.* 455 (2008) 376.
- [26] R. Naccache, F. Vetrone, V. Mahalingam, L.A. Cuccia, J.A. Capobianco, *Chem. Mater.* 21 (2009) 717.
- [27] F. Liu, E. Ma, D.Q. Chen, Y.S. Wang, Y.L. Yu, P. Huang, *J. Alloys Compd.* 467 (2009) 317.